

SANDIA REPORT

SAND2021-8053

Printed July 2021



Sandia
National
Laboratories

Shock and Reaction in Granular Bed of HMX-Aluminum Powders

Marcia A. Cooper

Prepared by
Sandia National Laboratories
Albuquerque, New Mexico 87185
Livermore, California 94550

Issued by Sandia National Laboratories, operated for the United States Department of Energy by National Technology & Engineering Solutions of Sandia, LLC.

NOTICE: This report was prepared as an account of work sponsored by an agency of the United States Government. Neither the United States Government, nor any agency thereof, nor any of their employees, nor any of their contractors, subcontractors, or their employees, make any warranty, express or implied, or assume any legal liability or responsibility for the accuracy, completeness, or usefulness of any information, apparatus, product, or process disclosed, or represent that its use would not infringe privately owned rights. Reference herein to any specific commercial product, process, or service by trade name, trademark, manufacturer, or otherwise, does not necessarily constitute or imply its endorsement, recommendation, or favoring by the United States Government, any agency thereof, or any of their contractors or subcontractors. The views and opinions expressed herein do not necessarily state or reflect those of the United States Government, any agency thereof, or any of their contractors.

Printed in the United States of America. This report has been reproduced directly from the best available copy.

Available to DOE and DOE contractors from

U.S. Department of Energy
Office of Scientific and Technical Information
P.O. Box 62
Oak Ridge, TN 37831

Telephone: (865) 576-8401
Facsimile: (865) 576-5728
E-Mail: reports@osti.gov
Online ordering: <http://www.osti.gov/scitech>

Available to the public from

U.S. Department of Commerce
National Technical Information Service
5301 Shawnee Road
Alexandria, VA 22312

Telephone: (800) 553-6847
Facsimile: (703) 605-6900
E-Mail: orders@ntis.gov
Online order: <https://classic.ntis.gov/help/order-methods>



ABSTRACT

Ignition and material response properties of aluminized HMX heterogeneous explosive mixtures were explored in a series of planar impact experiments performed over multiple years. This work expands on previous work studying material response to impact in single-component HMX granular materials. The addition of nanometric aluminum is shown to affect the ignition sensitivity and growth to reaction from impact. The gas gun test results are presented here varying parameters of particle size, shock strength, and aluminum mass fraction.

ACKNOWLEDGMENT

The authors gratefully acknowledge the experimental contributions and mentorship of Wayne Trott. Experimental data in this report were generated in the early 2000's by investigators: Wayne Trott (retired), Robert Pahl (now at Medtronic in Louisville, CO), and Marcia Cooper. John Liwski is gratefully acknowledged for executing the gas gun tests. Heidi Anderson is gratefully acknowledged for construction of the target assemblies. Sandia National Laboratories is a multimission laboratory managed and operated by National Technology and Engineering Solutions of Sandia, LLC, a wholly owned subsidiary of Honeywell International, Inc., for the U.S. Department of Energy's National Nuclear Security Administration under contract DE-NA-0003525.

CONTENTS

1. Introduction	7
2. Experiment	9
3. Shock Response: Particle Size Effects	13
4. Shock Response: Shock Strength Effects	17
5. Detonation Response: Aluminum Mass Fraction Effects	18
6. Conclusion	21
References	22

LIST OF FIGURES

Figure 2-1. Illustration of gas gun projectile and target assembly.	9
Figure 2-2. SEM Images of HMX (A) 106-150 μm and (B) 212-300 μm	10
Figure 2-3. SEM images of HMX and Al mixture. HMX 212-300 μm and 123 nm Al mixed by Hexane.	10
Figure 3-1. Plot of particle velocity histories for neat HMX powders with different particle sizes. Pellets pressed to 68% TMD.	13
Figure 3-2. Plot of particle velocity histories for neat HMX and HMX-aluminum powders. Impact velocity of 0.45 km/s. HMX particles between 212-300- μm and 68% TMD.	14
Figure 3-3. Plot of particle velocity histories for 106-150- μm HMX particles and the effect of aluminum loading. Impact velocity of 0.44 km/s. Pellets pressed to 68% TMD.	15
Figure 4-1. Plot of particle velocities for HMX-aluminum mixtures. HMX particle sizes between 212-300 μm , nanometric aluminum particle sizes and 68% TMD. Impact velocities vary from 0.45 to 1.21 km/s.	17
Figure 4-2. Particle velocity histories from Fig. 4-1 annotated with the start and slope change that occurs with the start of chemical decomposition.	18
Figure 4-3. Plot of time delay until the start of chemical decomposition versus post-shock particle velocity.	19
Figure 4-4. Plot of particle velocities for HMX-aluminum mixtures. HMX particle sizes between 106-150 μm , nanometric aluminum particle sizes and 68% TMD. Impact velocities vary from 0.44 to 0.77 km/s.	19
Figure 4-5. Particle velocity histories from Fig. 4-4 annotated with the start and slope change that occurs with the start of chemical decomposition.	20
Figure 5-1. Plot of particle velocities for HMX-aluminum mixtures containing 10, 20, and 30% aluminum nanoparticles by weight.	20

1. INTRODUCTION

The shock behavior of heterogeneous materials depends on the complex processes of material deformation and chemical reaction that occur over a range of micro- and macroscopic length scales. While chemical reaction, shock-induced phase changes, and dynamic yielding occur at microscopic length scales, it is the processes occurring at macroscopic length scales, corresponding to grain size dimensions, which are believed to have a dominant influence on shock response [2, 16, 18, 7]. Previous work on low-density pressings of explosive powders has yielded insight into the material shock response and the parameters affecting ignition and sustained reaction in neat powders [7].

Through a combination of experiments and mesoscale modeling, theories about the formation and role of hotspots, particle deformations due to high stress and shear forces, and the stochastic nature of the transmitted wave have been developed [18, 17, 15]. In particular, mesoscale modeling reveals that rapid deformation occurs at material contact points in such pressings subjected to impact. Localization effects first occur at these contact points, and subsequently, plastic flow into the interstitial pores produces localized regions, or “hotspots,” of sustained elevated temperature. Both stress and temperature fields display a substantial degree of large amplitude fluctuations. Wave profiles generated by these materials can exhibit distinct ordered wave structures that are distributed over multiple grain dimensions and often coherent temporally.

In this study, binary mixtures of HMX and aluminum particles were pressed to 68% of theoretical maximum density (TMD) and subjected to planar shock loading using a gas gun and projectile. The particles were ultrasonically mixed in a solvent such that the added micron-sized or nanometric aluminum powder tended to coat the explosive grains once the solvent was evaporated. This morphology is thought to promote rapid exposure of the metal additive to both material deformation and sustained elevated temperatures under shock loading. The former process is likely useful in stripping surface oxide from the metal while the latter condition may be expected to promote aluminum chemistry. Finally, the use of low-density samples (with minimal grain fracture during pressing) is helpful in defining a material geometry that can be reasonably approximated in mesoscale numerical simulations. Planar impact loading of low-density pressings of the neat HMX have been shown to respond to modest shock loading by developing distinctive reactive waves that exhibit both temporal and mesoscale spatial fluctuations [16, 18]. We extend the previous work with neat HMX pellets to include micron-sized and nanometric aluminum particles aimed to further advance our understanding of material response in binary mixtures. Velocity interferometry was used to explore the effect of variations in impact velocity and aluminum particle size and mass fraction.

2. EXPERIMENT

Testing was performed in a single-stage gas gun with an 18-meter-long barrel, which drove an aluminum projectile at a velocity between 0.3 km/s and 1.2 km/s into a target assembly containing the explosive pellet. The projectile and target assembly are illustrated in Fig. 2-1. The 6.35-cm-diameter aluminum projectile contained a Kel-F impactor that contacted the target assembly. The impact face of the target assembly consisted of a Kel-F sample cup containing the explosive pellet, which was aligned onto the gas gun barrel with the target cup. A series of eight time-of-arrival pins located around the circumference of the impact face were used to obtain an accurate measurement of the projectile velocity and tilt immediately before impact. The 0.4-mm-thick pressed explosive was confined in the sample cup by a buffer layer of Kapton and an aluminized polymethyl methacrylate (PMMA) interferometer window. The aluminum layer on the PMMA window was 12.7- μm thick and the Kapton buffer was 225- μm thick. The Kapton buffer layer was necessary to avoid severe loss in reflected light intensity when the aluminized window was placed in direct contact with the pressed pellet [18]. The explosive material was pressed into the sample cup using pressing fixtures machined to a tolerance of ± 0.025 mm.

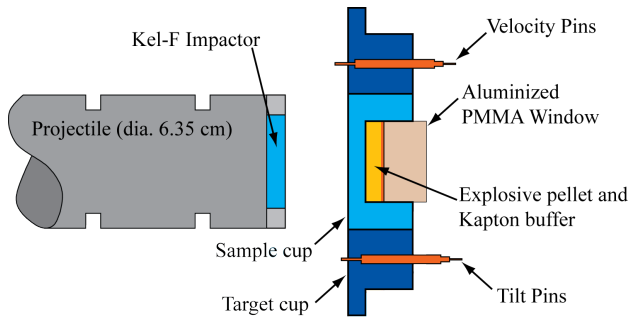


Figure 2-1 Illustration of gas gun projectile and target assembly.

The HMX was taken from a 106-150 μm or 212-300- μm sieve cut from Grade B, class 1 HMX produced by Holston. The two aluminum particle sizes, both with spherical morphology, used in these tests were 2 μm (H-2 produced by Valimet) and 123 nm (produced by Technanogy) or 120 nm (produced by Nanotechnologies). Unless specifically noted, the pellets consisted of 10% aluminum particles by mass and the presence of the oxide layer was not accounted for in the mass measurements.

To ensure dispersion of the aluminum powder throughout the mixture, the aluminum was first mechanically mixed with the HMX powder and then ultrasonically agitated in hexane for several minutes. SEM images of pellets pressed from this mixture have shown adequate dispersal of Al with minimal agglomeration [14]. In all HMX/Al test cases, the targets were pressed to a nominal density of 68% TMD. The density difference between Al and Al₂O₃ and the particle mass fraction of the oxide were accounted for in the target density calculations.

A dual-delay-leg, “push-pull” VISAR diagnostic for single-point measurements was used. Additional details about the VISAR system are in Lederer et al. [11]. The velocity-time history is obtained from the measured fringe data by determining the instantaneous phase angle and multiplying by the Velocity per Fringe (VPF) constants of 0.7574 km/s/fr or 0.2023 km/s/fr for

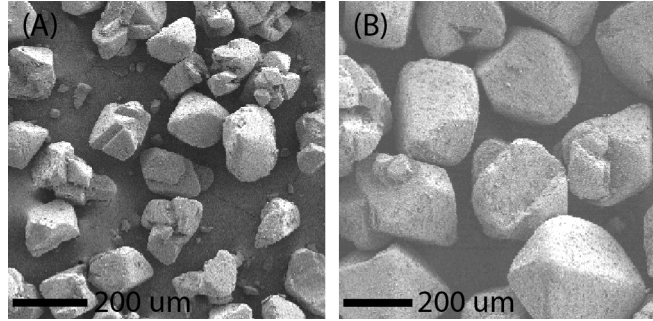


Figure 2-2 SEM Images of HMX (A) 106-150 μm and (B) 212-300 μm .

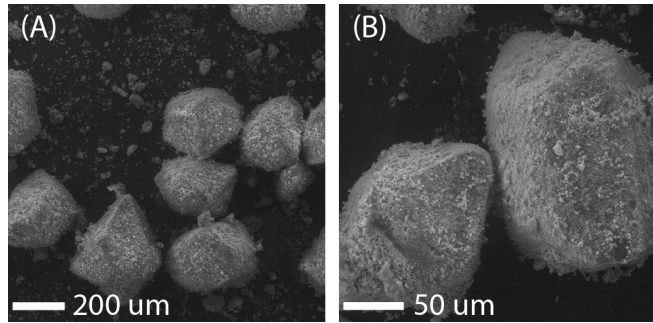


Figure 2-3 SEM images of HMX and Al mixture. HMX 212-300 μm and 123 nm Al mixed by Hexane.

the first leg and 0.2823 km/s/fr for the second leg. The velocity data for both legs of the VISAR system are matched by adding or removing fringes until a unique solution for the velocity is determined.

In all cases, the VISAR profiles show the particle velocity of the aluminum surface at the interface between the Kapton buffer and the PMMA window. After projectile impact, a shock wave is transmitted into the pellet which compresses the sample. As this compaction wave propagates through the sample, some or all of the bed porosity is removed and grain crushing at particle boundaries may occur for significantly high shock pressures. This propagating compaction wave can be more or less dispersive depending on particle sizes, pressed density and impact velocity. Once the compaction wave reaches the aluminized surface of the PMMA window, an increase in particle velocities behind this compaction wave is recorded by the VISAR diagnostic. In some cases, the temporal variations in the post-compaction wave particle velocities have been correlated to several dominant frequencies that correspond to the grain size dimensions [18]. In addition to temporal variations in particle velocities, spatial variations have also been observed across a pellet with the ORVIS diagnostic [17]. For low shock strengths, energy release from HMX decomposition reactions do not extensively start at the shock front [17, 8]. If extensive decomposition reactions do occur at the shock front, a decreasing stress and particle velocity immediately behind the shock front is observed [16, 8, 9]. The VISAR data of particle velocities persists until corrupted by the relief waves from the sample side boundary.

The VISAR time histories are exclusively used in the subsequent sections to assess shock and ignition in powder pressings of HMX and aluminum mixtures. Parameters of aluminum mass

fraction, aluminum and HMX particle sizes, and impact velocity are presented.

3. SHOCK RESPONSE: PARTICLE SIZE EFFECTS

The effect of particle size on the material response from shock has been previously documented in single-component particle mixtures [18, 17, 16]. At low impact velocities where reaction does not occur, increasing the particle size results in an increase in the spatial and temporal wave dispersion. When chemical reaction does occur, the wave steepens as it travels. When chemical reaction does not occur, there is little dependence of the compaction wave on density at these low impact velocities. It is well established that a critical length scale based on the particle size determines the width of the compaction wave [16]. When chemical reaction does occur, increasing the density acts to reduce the sensitivity to shock initiation and early reaction growth.

The effect of HMX particle size for the same density and similar impact velocity appear in Fig. 3-1. The data for the larger particles were obtained by spatially averaging the ORVIS-measured particle velocities whereas the data for the smaller particles were obtained at a single point with the VISAR diagnostic. The finer particles cause a more dispersive compaction wave that arrives at the measurement surface nearly $1.5 \mu\text{s}$ later than the compaction wave in the larger particles. In both cases, the particle velocities remain relatively constant followed by a slight increase indicating that extensive reaction is not occurring at the shock front. For the smaller particles, a delay of approximately $1.75 \mu\text{s}$ occurs before extensive reactions cause the particle velocity to rapidly increase. An equivalently rapid increase in particle velocity is not observed for the large particles within the measurement time. Coarser materials have relatively large hot spots which lead to initiation at lower input pressures, whereas, hot spots formed in finer materials experience more rapid cooling such that their sensitivity is less than that of coarser materials.

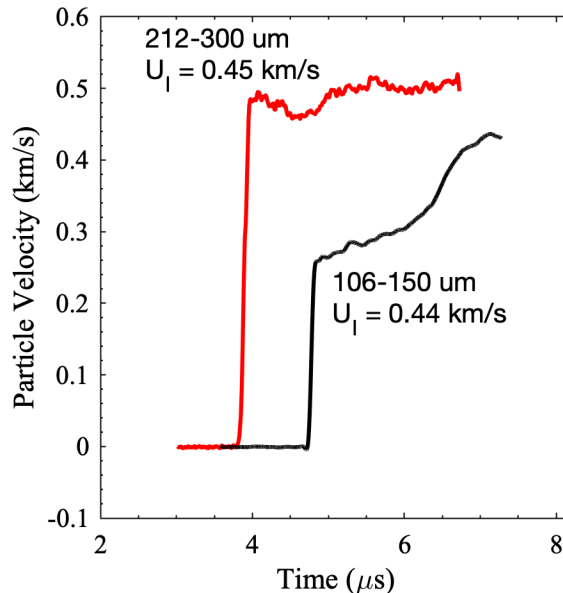


Figure 3-1 Plot of particle velocity histories for neat HMX powders with different particle sizes. Pellets pressed to 68% TMD.

The effect of aluminum size on the material response of HMX-aluminum mixtures is shown in Fig. 3-2 for impact velocities of approximately 0.45 km/s. In this plot, the size of the HMX particles remains constant between 212-300 μm . The addition of the smaller aluminum results in dramatic decreases in the particle velocities as compared to neat HMX. The compaction waves for the HMX-aluminum pellets arrive approximately 1 μs later than in the neat HMX case. Additionally, the time delay behind the shock front before evidence of extensive reaction is observed to be approximately 1.5 μs longer for the HMX-aluminum mixtures and increases as the aluminum particle size decreases. This indicates that the adding finely dispersed aluminum initially suppresses the energy release corresponding to HMX decomposition. This reaction suppression likely arises from a complex combination of physical factors including differences in shock impedance and particle size distribution as well as a probable reaction “bottleneck” due to the aluminum coating of the individual grains. The aluminum coating of the HMX grains is less uniform for the 2- μm aluminum particles likely due to >1000 x fewer particles for a given mass percent. A similar delay in reaction is observed in the smaller HMX particle sizes of Fig. 3-3.

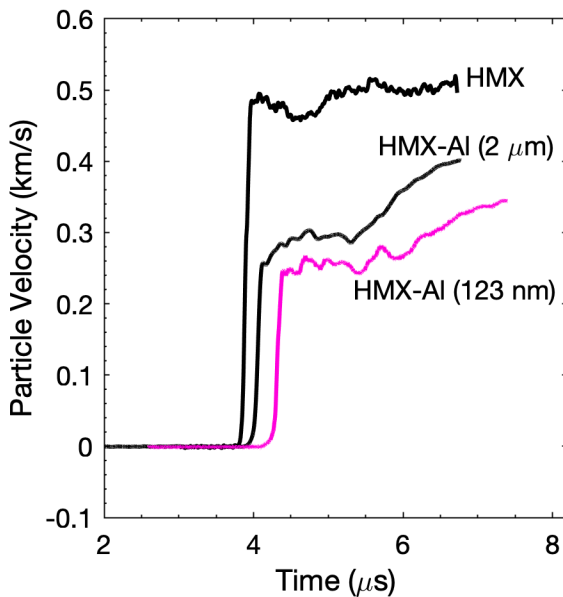


Figure 3-2 Plot of particle velocity histories for neat HMX and HMX-aluminum powders. Impact velocity of 0.45 km/s. HMX particles between 212-300- μm and 68% TMD.

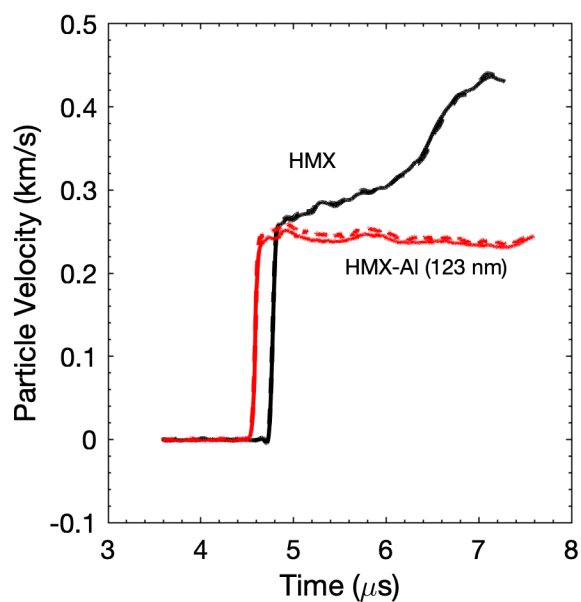


Figure 3-3 Plot of particle velocity histories for 106-150- μm HMX particles and the effect of aluminum loading. Impact velocity of 0.44 km/s. Pellets pressed to 68% TMD.

4. SHOCK RESPONSE: SHOCK STRENGTH EFFECTS

The effect of projectile velocity from 0.45 to 1.21 km/s for HMX-aluminum mixtures with HMX particle sizes between 212-300 μm at 68% TMD appears in Fig. 4-1. Tests with impact velocities below 0.8 km/s used 123 nm aluminum particles whereas tests with impact velocities greater than 0.8 km/s used 120 nm aluminum particles. Largely dispersive compaction waves are observed for the tests with impact velocities less than 0.56 km/s.

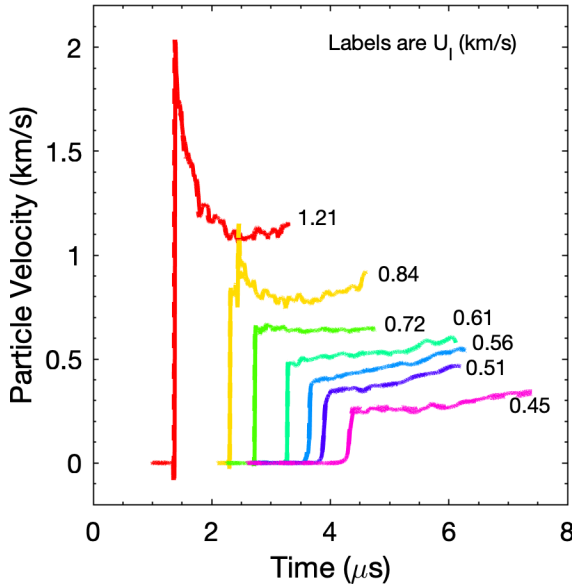


Figure 4-1 Plot of particle velocities for HMX-aluminum mixtures. HMX particle sizes between 212-300 μm , nanometric aluminum particle sizes and 68% TMD. Impact velocities vary from 0.45 to 1.21 km/s.

A delay time associated with the onset of extensive decomposition reactions appears in the data after arrival of the compaction wave and before arrival of the side relief wave. This delay time is most evident in the data associated with the four lowest impact velocities as shown in Fig. 4-2 as noted by the arrows. The temporal variations during the delay time are likely indicative of some decomposition and hotspot formation but significant loss mechanisms are affecting the reaction kinetics. At a critical distance behind the compaction wave, the decomposition kinetics become dominant and a relatively constant increase in particle velocity is observed until arrival of the side relief waves. The intersection point of two straight-line fits through the data of constant particle velocity and increasing particle velocity were used to determine the delay time at each impact velocity. The delay times for all impact velocities are compiled in Fig. 4-3. As the impact velocity increases, the delay time until the start of decomposition reactions decreases.

At an impact velocity of 0.720 km/s, the post-shock particle velocities appear constant. However, at approximately 3.38 μs (Fig. 4-1) a slight increase in the particle velocity occurs immediately followed by a modest particle velocity decrease. It is believed that at this impact velocity, the decomposition reactions are beginning to occur within the shock front. The data at an impact velocity of 0.843 km/s are interesting in that the shock results in particle velocities of

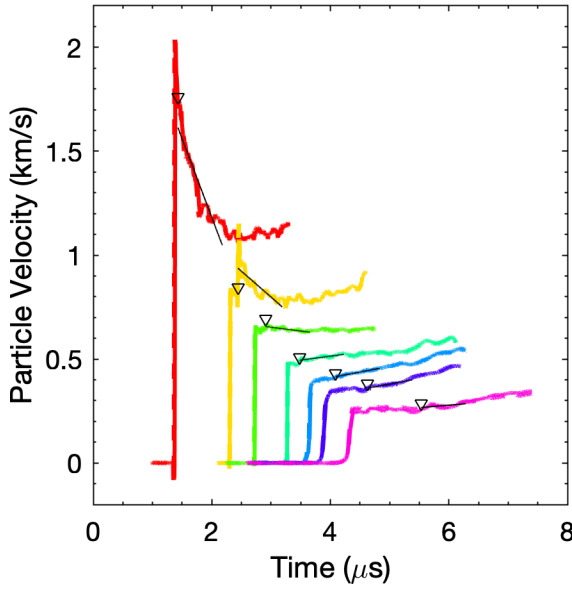


Figure 4-2 Particle velocity histories from Fig. 4-1 annotated with the start and slope change that occurs with the start of chemical decomposition.

approximately 0.8 km/s. After about $0.1 \mu\text{s}$ the particle velocity rapidly increases to a peak value of 1.2 km/s and then decreases with significant temporal fluctuations. The rapid spike in particle velocities can be attributed to intense chemical decomposition reactions. For materials with fine particles, the presence of rapid reaction has been observed in that they have a longer induction time or less sensitivity to initiation but upon initiation the rate of reaction is significantly greater than coarser materials [16].

The data at an impact velocity of 1.209 km/s shows the typical profile in which extensive decomposition reactions are occurring at the shock front followed by product expansion.

The reaction delay time is plotted in Fig. 4-3 along with the slope in the particle velocity after the start of reaction (e.g., the acceleration) as a function of the post-shock particle velocity.

Figure 4-4 plots the effect of projectile velocity from 0.44 to 0.77 km/s for HMX-aluminum mixtures with HMX particle sizes between 106-150 μm at 68% TMD.

5. DETONATION RESPONSE: ALUMINUM MASS FRACTION EFFECTS

Figure 5-1 plots the particle velocities for mixtures containing 10, 20 and 30% aluminum particles by weight. The mixtures consisted of 120-nm aluminum particles and HMX particles had sizes ranging between 212 and 300 μm . For each test, the particle velocity decreases immediately behind the transmitted wave indicating that reaction is occurring at the shock front. The addition of aluminum particles causes a delay in the arrival time of the transmitted wave and a decrease in the peak particle velocity. Note that an extended region of energy release is observed immediately

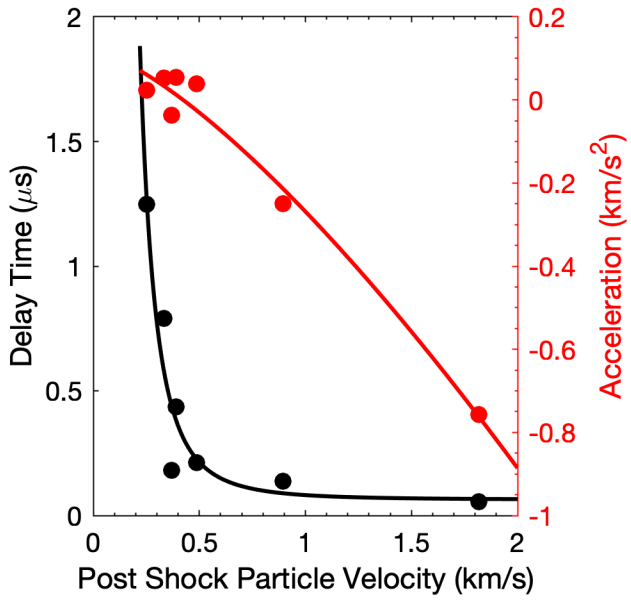


Figure 4-3 Plot of time delay until the start of chemical decomposition versus post-shock particle velocity.

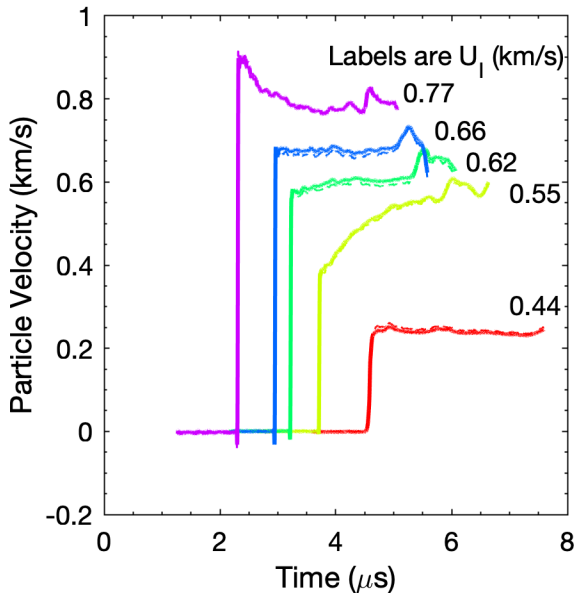


Figure 4-4 Plot of particle velocities for HMX-aluminum mixtures. HMX particle sizes between 106-150 μ m, nanometric aluminum particle sizes and 68% TMD. Impact velocities vary from 0.44 to 0.77 km/s.

after the transmitted wave and the extent of this region appears to grow as the amount of aluminum increases.

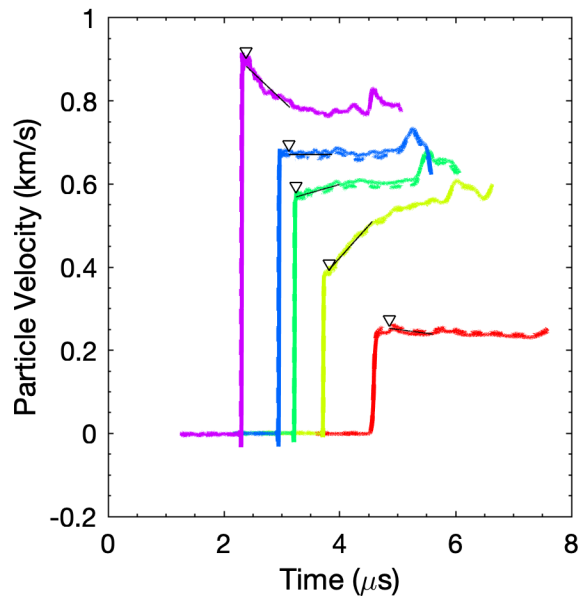


Figure 4-5 Particle velocity histories from Fig. 4-4 annotated with the start and slope change that occurs with the start of chemical decomposition.

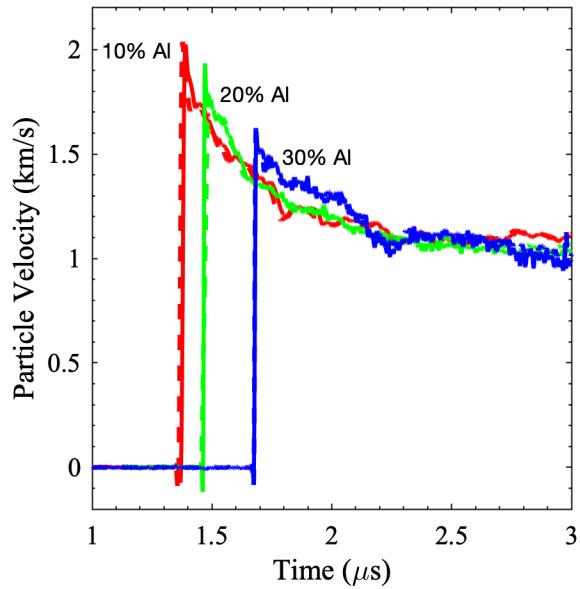


Figure 5-1 Plot of particle velocities for HMX-aluminum mixtures containing 10, 20, and 30% aluminum nanoparticles by weight.

6. CONCLUSION

The data shown here indicate that under low density, moderate loading conditions, the presence of aluminum particles can affect the post-compaction wave porosity and material state. Aluminum acts to delay the onset of extensive chemical reaction at low impact conditions, yet above critical impact loadings the fine aluminum particles can cause rapid reaction similar to that seen in pressings of fine particles. At near-detonation conditions, post-shock particle velocities indicate that the aluminum may not be entirely participating in reactions at the shock front but rather immediately following the shock front.

REFERENCES

- [1] Tim Bazyn, Herman Krier, and Nick Glumac. Shock tube measurements of combustion of nano-aluminum. In *44th AIAA Aerospace Sciences Meeting and Exhibit*, Reno, NV, January 9-12, 2006. AIAA 2006-1157.
- [2] F. P. Bowden and A. D. Yoffe. *Initiation and Growth of Explosion in Liquids and Solids*. Cambridge University Press, 1952.
- [3] Aaron Brundage. Personal communication, 2007.
- [4] Joel R. Carney, J. Scott Miller, Jared C. Gump, and G. I. Pangilinan. Time-resolved optical measurements of the post-detonation combustion of aluminized explosives. *Review of Scientific Instruments*, 77:063103 – 063103–6, 2006.
- [5] P. W. Cooper. *Explosives Engineering*. Wiley-VCH, Inc., New York, NY, 1996.
- [6] CVI Laser. Optical filters specifications, 2008.
- [7] J. J. Dick. Measurement of the shock initiation sensitivity of low density hmx. *Combustion and Flame*, 54:121–129, 1983.
- [8] J. J. Dick. Stress-time profiles in low density hmx. *Combustion and Flame*, 69:257–262, 1987.
- [9] Wildon Fickett. Shock initiation of detonation in a dilute explosive. *Physics of Fluids*, 27(1):94–105, 1984.
- [10] S. D. Gilev and V. F. Anisichkin. Interaction of aluminum with detonation products. *Combustion, Explosion, and Shock Waves*, 42(1):107–115, 2006.
- [11] R. A. Lederer, S. A. Sheffield, A. C. Schwarz, and D. B. Hayes. In *Proceedings of the Sixth Symposium International on Detonation*, page 668, 1976. Report No. ACR-221.
- [12] Ralph Menikoff. Compaction wave profiles: Simulations of gas gun experiments. *Journal of Applied Physics*, 90(4):1754–1760, August 2001.
- [13] J. Scott Miller and G. I. Pangilinan. Measurements of aluminum combustion in energetic formulations. In M. D. Furnish, Y. M. Gupta, and J. W. Forbes, editors, *Shock Compression of Condensed Matter*, pages 867–870. American Institute of Physics, 2003.
- [14] Robert J. Pahl, Wayne M. Trott, Jaime N. Castaneda, Stephen K. Marley, and Shane Snedigar. Evaluation of aluminum participation in the development of reactive waves in shock compressed hmx. In *13th International Detonation Symposium*, Norfolk, VA, July 23-28, 2006.
- [15] S. A. Sheffield, D. D. Bloomquist, and C. M. Tarver. Subnanosecond measurements of detonation fronts in solid high explosives. *Journal of Chemical Physics*, 80(8):3831–3844, April 1984.

- [16] S. A. Sheffield, R. L. Gustavsen, and M. U. Anderson. *Shock Loading of Porous High Explosives*, chapter 2, pages 23–61. High-Pressure Shock Compression of Solids IV. Springer-Verlag, New York, NY, 1997.
- [17] Wayne M. Trott, Melvin R. Baer, Jaime N. Castaneda, Lalit C. Chhabildas, and James R. Asay. Investigation of the mesoscopic scale response of low-density pressings of granular sugar under impact. *Journal of Applied Physics*, 101:024917–1 – 024917–21, 2007.
- [18] Wayne M. Trott, Jaime N. Castaneda, John J. O'Hare, Melvin R. Baer, Lalit C. Chhabildas, Marcus D. Knudson, Jean-Paul Davis, and James R. Asay. Dispersive velocity measurements in heterogeneous materials. Technical Report SAND2000-3082, Sandia National Laboratories, Albuquerque, New Mexico, USA, December 2000.
- [19] Sergey B. Victorov. The effect of al₂o₃ phase transitions on detonation properties of aluminized explosives. August 11-16, 2002. 12th Int. Detonation Symp., Aug 11-16.
- [20] Shfeng Wang, Yanqiang Yang, Zhaoyong Sun, and Dana D. Dlott. Fast spectroscopy of energy release in nanometric explosives. *Chemical Physics Letters*, 368:189–194, 2003.

DISTRIBUTION

Email—Internal

Name	Org.	Sandia Email Address
Shane Schumacher	1555	scschum@sandia.gov
Michael Kaneshige	7500	mjkanes@sandia.gov
Alex Tappan	7554	astappa@sandia.gov
Technical Library	1911	sanddocs@sandia.gov



**Sandia
National
Laboratories**

Sandia National Laboratories is a multimission laboratory managed and operated by National Technology & Engineering Solutions of Sandia LLC, a wholly owned subsidiary of Honeywell International Inc., for the U.S. Department of Energy's National Nuclear Security Administration under contract DE-NA0003525.